Alignment of Lamellar Block Copolymer Microstructure in an Electric Field. 1. Alignment Kinetics

Karl Amundson,* Eugene Helfand, and Xina Quan

AT&T Bell Laboratories, Murray Hill, New Jersey 07974

Steven D. Smith

The Procter and Gamble Company, Cincinnati, Ohio 45239

Received November 16, 1992; Revised Manuscript Received February 12, 1993

ABSTRACT: The kinetics of alignment of block copolymer microstructure in an electric field has been studied. The rate of alignment obeys a simple time–temperature–field superposition law when thermal history is well-controlled. Thermal history also strongly affects the alignment rate. We propose that observed trends can be understood in terms of mechanisms of defect movement and pinning.

I. Introduction

A number of investigations have shown that block copolymer microstructure can be aligned by surfaces or flow.[1-8] We have studied the alignment of block copolymer microstructure in an electric field.[9] Alignment by an electric field offers the possibility of producing block copolymer materials with "tailored" anisotropic properties; e.g., spatially-specific anisotropic properties could be imposed by a localized electric field. In addition, the response of block copolymer microstructure to a body force, such as is provided by an electric field, should reveal large-scale properties of block copolymer materials like defect mobility. Recently, we reported on the alignment of block copolymer microstructure by cooling samples through the order–disorder transition (ODT) in the presence of an electric field.[9] In this and a companion paper,[10] we focus on alignment of block copolymer microstructure solely in the ordered state.

A. Electrothermodynamics. The free energy of a dielectric material in an electric field is

$$\mathcal{F} = \mathcal{F}_0 - \frac{1}{8\pi}\int_{\mathcal{V}} \epsilon(\mathbf{r})|\mathbf{E}(\mathbf{r})|^2 \, d^3\mathbf{r} \tag{1.1}$$

for the condition of constant-potential boundaries.[11] $\mathcal{F}$ is the free energy, $\mathcal{F}_0$ the free energy without an electric field, $\epsilon(\mathbf{r})$ the local dielectric constant, and $\mathbf{E}(\mathbf{r})$ the electric field. The integration is over the volume of the material, $\mathcal{V}$. Different composition patterns within a block copolymer material and the associated spatially-varying local dielectric constant produce different patterns of electric field. The consequence is a composition-pattern-dependent electrostatic contribution to the free energy. Certain orientations of the composition pattern are thermodynamically favored over others. An expression for the electrostatic contribution to the free energy in terms of the composition pattern is derived next.

The local dielectric constant in a block copolymer sample is a function of the local composition. It is convenient to expand about the condition of vanishing amplitude of the composition pattern:

$$\epsilon(\mathbf{r}) = \epsilon_D(\mathbf{r}) + \beta\bar{\psi}(\mathbf{r}) + \frac{1}{2}\frac{\partial^2\epsilon}{\partial\psi^2}[\bar{\psi}(\mathbf{r})]^2 \tag{1.2}$$

to second order in the composition pattern, $\bar{\psi}(\mathbf{r})$. ϵ_D is the dielectric constant in the limit of vanishing stationary composition pattern and includes effects of dynamic composition fluctuations.[12] $\psi(\mathbf{r})$ is the local volume fraction of one component minus its mean value. $\bar{\psi}(\mathbf{r})$ is the compositional pattern associated with the ordered state; the bar denotes a time average over a scale much greater than fluctuation lifetimes but much less than the time of evolution of the composition pattern.[13] β measures the sensitivity of the dielectric constant to composition change: $\beta = \partial\epsilon/\partial\psi$.

The electric field obeys the Maxwell equation $\nabla\cdot[\epsilon(\mathbf{r})\mathbf{E}(\mathbf{r})] = 0$. This equation is readily solved by Fourier transform and perturbation of $\bar{\psi}(\mathbf{r})$ about zero. The Fourier transform of the electric field is given to first order by

$$\tilde{\mathbf{E}}(\mathbf{k}) = \left[\underline{I} - \frac{\beta}{\epsilon_D}\tilde{\bar{\psi}}(\mathbf{k})\hat{\mathbf{e}}_k\hat{\mathbf{e}}_k\right]\cdot\mathbf{E}_0 \tag{1.3}$$

$\hat{\mathbf{e}}_k$ is the unit wave vector and $\tilde{\bar{\psi}}(\mathbf{k})$ is the Fourier transform of $\bar{\psi}(\mathbf{r})$. Inserting this and eq 1.2 into eq 1.1 gives the electrostatic contribution to the free energy:

$$\mathcal{F} - \mathcal{F}_0 = \frac{1}{8\pi}\epsilon_D|\mathbf{E}_0|^2\left[-\left(\frac{\langle\epsilon\rangle}{\epsilon_D}\right)\mathcal{V} + \left(\frac{\beta}{\epsilon_D}\right)^2\frac{1}{(2\pi)^3}\int\tilde{\bar{\psi}}(\mathbf{k})\tilde{\bar{\psi}}(-\mathbf{k})(\hat{\mathbf{e}}_k\cdot\hat{\mathbf{e}}_z)^2\,d^3\mathbf{k}\right] \tag{1.4}$$

to second order in the stationary composition pattern. The integral is over the wave vector conjugate to the space vector $\mathbf{r}$. $\hat{\mathbf{e}}_z$ the unit vector in the direction of the applied field, $\mathbf{E}_0$. It can be shown that the second-order term in the electric field does not contribute to the free energy to second order because the electric field to each order can be written as the gradient of a scalar potential. The free energy expression neglects as small the contribution to the electric field energy from the alignment and stretching of chains and the difference of polarizability of these chains in the directions along and perpendicular to the bonds. Such effects were recently considered in the context of birefringence by Lodge and Fredrickson[14] (see discussion after eq 1.9). $\langle\epsilon\rangle$ is given by

$$\langle\epsilon\rangle = \epsilon_D + \frac{1}{2}\left(\frac{\partial^2\epsilon}{\partial\psi^2}\right)\langle\bar{\psi}^2\rangle \tag{1.5}$$

where the angular brackets denote a space average. The second term represents the change in the space-average dielectric constant from ϵ_D due to material separation. The first term on the right of the free energy expression, eq 1.4, is just the electrostatic energy for a material with the space-averaged dielectric constant given by $\langle\epsilon\rangle$. This term is isotropic and so does not contribute an aligning force.

0024-9297/93/2226-2698$04.00/0

The second term on the right of eq 1.4 can yield an anisotropic contribution to the free energy of the ordered state and is the basis for electric field alignment. At this point, let us consider the aligning force on various block copolymer microstructures. For microstructures with at least two distinct axes of threefold or greater rotational symmetry, the integral of eq 1.4 is isotropic, and the electric field cannot act to align the microstructure. In this class are the body-centered cubic (spherical) and the ordered bicontinuous double-diamond microstructures.

On the other hand, cylindrical and lamellar microstructures do interact anisotropically with an electric field. Since the anisotropic electric energy term is nonnegative, it is minimized by orientations for which the Fourier components making up the pattern have wave vectors orthogonal to the applied field. The cylindrical morphology, in weak segregation, is made up of Fourier components with six coplanar, hexagonally-arranged wave vectors. From eq 1.4, the electric field contribution to the free energy density is

$$\frac{\mathcal{F}-\mathcal{F}_0}{\mathcal{V}} = \frac{1}{8\pi}\epsilon_D|\mathbf{E}_0|^2\left[\frac{1}{2}\left(\frac{\beta}{\epsilon_D}\right)^2\langle\bar{\psi}^2\rangle[1-(\hat{\mathbf{e}}_c\cdot\hat{\mathbf{e}}_z)^2]-\frac{\langle\epsilon\rangle}{\epsilon_D}\right] \tag{1.6}$$

where we made use of the relation

$$\frac{1}{(2\pi)^3\mathcal{V}}\int\tilde{\psi}(\mathbf{k})\,\tilde{\psi}(-\mathbf{k})\,d^3\mathbf{k} = \langle[\bar{\psi}(\mathbf{r})]^2\rangle \tag{1.7}$$

$\hat{\mathbf{e}}_c$ is the unit vector in the direction of the cylindrical axes. The free energy is minimized for any orientation where the six wave vectors are in the plane perpendicular to an applied field; i.e., the cylindrical axes are parallel to the field.

In this paper, the materials under consideration exhibit a lamellar microstructure. The wave vectors of the Fourier components making up this microstructure are antiparallel. The free energy is minimized when the wave vectors are in the plane perpendicular to $\mathbf{E}$; that is, the lamellar planes contain $\mathbf{E}$. Note that this condition does not specify a single minimum-energy orientation, but a set of states along a ring. From eq 1.4, the electric contribution to the free energy density for a lamellar morphology is

$$\frac{\mathcal{F}-\mathcal{F}_0}{\mathcal{V}} = \frac{1}{8\pi}\epsilon_D|\mathbf{E}_0|^2\left[\left(\frac{\beta}{\epsilon_D}\right)^2\langle\bar{\psi}^2\rangle(\hat{\mathbf{e}}_q\cdot\hat{\mathbf{e}}_z)^2-\frac{\langle\epsilon\rangle}{\epsilon_D}\right] \tag{1.8}$$

Here, $\hat{\mathbf{e}}_q$ is the unit wave vector of the lamellar pattern. Only the first term in the brackets is anisotropic and contributes toward alignment. The force of alignment is proportional to the applied field strength squared, $|\mathbf{E}_0|^2$, the mean-square of the composition pattern strength, $\langle\bar{\psi}^2\rangle$, and the material parameter β^2/ϵ_D.

The size of the anisotropic component of the electric energy is rather small. To put it on a relative basis, for the energy difference between aligned and misaligned orientations of a region to equal k_BT (k_B is Boltzmann's constant, T is temperature), the region must be of the order of a couple of hundred nanometers on a side (for the material and field strengths of this work). Only because the electric field is acting on an organized state with long-range order does it have important effects.

B. Birefringence and Alignment of Microstructure. The ordered phase of a block copolymer sample has form birefringence. In a material with uniform microstructure, the effective dielectric tensor is given by

$$\underline{\epsilon} = \langle\epsilon\rangle\underline{I} - \frac{\beta^2}{\epsilon_D}\langle\bar{\psi}^2\rangle\hat{\mathbf{e}}_q\hat{\mathbf{e}}_q \tag{1.9}$$

to second order in the composition pattern.[15] All dielectric constants and β must be evaluated at the frequency of light when computing birefringence, and so they are different from those used in equations relating to electrothermodynamics. Equation 1.9 neglects the anisotropy of the dielectric tensor resulting from the alignment, in an inhomogeneous distribution of components, of bonds that have different polarizability in different directions. Such anisotropy leads to what is called intrinsic birefringence. Lodge and Fredrickson[14] have calculated that the intrinsic birefringence is about one-third of the form birefringence for the block copolymer of this study, but in strong segregation. We have estimated that the ratio of the intrinsic to form birefringence is about the same in weak segregation, although both are down by a factor of $\langle\bar{\psi}^2\rangle$.

While the evolution of light polarization upon passage through a uniformly birefringent material is relatively simple,[16,17] it is much more complicated when the birefringence is spatially varying. Some simplification comes from the smallness of the birefringence of block copolymers. Propagation through a globally disordered block copolymer material with lamellar microstructure was characterized in recent publications.[15,18-20] In the limit of large coherence length of the microstructure pattern, or "grain size", compared to the wavelength of light, a ray picture is appropriate. The state of polarization of the rays is conveniently represented as points on a Poincaré sphere, and evolution of the light polarization state during passage through a statistical distribution of grains corresponds to a set of random walks on the Poincaré sphere.[15] The evolution of the state of light polarization can, to an approximation, be considered as a series of rotations associated with passage through various "regions of coherence"[21] within the sample. Since the various rotations do not commute, the spatial arrangement of coherent regions is important. However, if the rotations are small, their noncommutativity (which contribute in second order) is very small. In fact, this is the case, as is shown next. Finally, it should be noted that when the grain size is on the order of the wavelength of light, interference effects can become very important and a scheme other than the ray picture needs to be adopted.

The magnitude of the rotation of the state of light polarization upon passage through a region of coherence is

$$\delta = 2\pi\frac{l}{\lambda}\Delta n^0\overline{\langle\psi\rangle^2}\sin^2\gamma \tag{1.10}$$

where l is the optical path length, λ is the wavelength of light in the medium (420 nm for 633-nm He–Ne laser light), and Δn^0 is given in eq 1.15. γ is the angle between the unique optical axis and the optical propagation direction. From transmission electron micrographs, the length of a coherent region is typically on the order of 5 μm. Using $\langle\bar{\psi}\rangle^2 \sim 0.13$, a typical single rotation is on the order of 0.02 rad. Since this is small, the tremendous simplification of ignoring the noncommutativity of the various rotations is adopted. The evolution of light polarization upon passage through the material is then approximated as that for passage through a material with the space-average dielectric tensor:

$$\langle\underline{\epsilon}\rangle = \langle\epsilon\rangle\underline{I} - \frac{\beta^2}{\epsilon_D}\langle\bar{\psi}^2\rangle\langle\hat{\mathbf{e}}_q\hat{\mathbf{e}}_q\rangle \tag{1.11}$$

In the case of a sample aligned by an electric field, one expects the distribution of lamellar normal vectors to be symmetric about the field direction, $\hat{\mathbf{e}}_z$. In this case, this

equation yields the effective dielectric tensor

$$\langle \underline{\epsilon} \rangle = \left[\langle \epsilon \rangle - \frac{1}{3}\frac{\beta^2}{\epsilon_D}\langle \bar{\psi}^2 \rangle \right] \underline{I} - \frac{2}{3}\frac{\beta^2}{\epsilon_D}\langle \bar{\psi}^2 \rangle S \left(\frac{3}{2}\hat{\mathbf{e}}_z\hat{\mathbf{e}}_z - \frac{1}{2}\underline{I} \right) \tag{1.12}$$

S is the orientational order parameter:

$$S = \frac{3}{2}\langle \cos^2 \theta \rangle - \frac{1}{2} \tag{1.13}$$

where θ is the angle between $\hat{\mathbf{e}}_q$ and $\hat{\mathbf{e}}_z$. For a macroscopically disordered block copolymer sample, S will be zero. S decreases during electric field alignment, and for maximum alignment in the field S will be $-1/2$. This is the condition where $\hat{\mathbf{e}}_q$ is everywhere orthogonal to $\hat{\mathbf{e}}_z$.

For propagation of light in an arbitrary direction (not along one of the eigenvectors of $\langle \underline{\epsilon} \rangle$), double refraction occurs, and light propagation cannot be characterized as plane wave propagation.[16] However, since the ratio of the anisotropic to isotropic component of $\langle \underline{\epsilon} \rangle$ is bounded by $\beta/\epsilon_D^2\langle \bar{\psi}^2 \rangle$, which is small ($\sim 10^{-2}$), light propagation will be approximated simply as a plane wave. The effective birefringence for light propagating at an angle α with respect to $\hat{\mathbf{e}}_z$ is then

$$\Delta n \doteq \Delta n^0 \langle \bar{\psi}^2 \rangle S \sin^2 \alpha \tag{1.14}$$

where

$$\Delta n^0 = -\frac{(n_1^2 - n_2^2)^2}{2n_D^3} \tag{1.15}$$

(for small $(\beta/\epsilon_D)^2\langle \bar{\psi}^2 \rangle$). Here, β is approximated as $(\epsilon_1 - \epsilon_2) \equiv (n_1^2 - n_2^2)$, where the subscripts "1" and "2" refer to properties of the two pure components. n_D is the square root of ϵ_D. The fast optical axis is along the projection of $\hat{\mathbf{e}}_z$ onto the plane perpendicular to the light propagation direction. From refractive index data for polystyrene and poly(methyl methacrylate) reported by Michel et al.,[22] Δn^0 for a symmetric polystyrene-*b*-poly(methyl methacrylate) copolymer is computed to be -4.0×10^{-3} at 160 °C and is expected to drop only slightly ($\sim 6\%$) upon heating to 260 °C. Equation 1.14 shows that the birefringence is proportional to the orientational order parameter, S. For alignment induced by a vertical electric field and a horizontal optical path, α equals 90°, and the birefringence relates to S as

$$\Delta n \doteq \Delta n^0 \langle \bar{\psi}^2 \rangle S \tag{1.16}$$

II. Experimental Section

Two polystyrene–poly(methyl methacrylate) diblock copolymer samples were synthesized anionically. Their molecular weight averages are 37 000 and 31 000 (polydispersity index 1.08 and 1.07, respectively), and they are referred to as SM-37 and SM-31, respectively. Both copolymers are 53 vol % polystyrene as determined by ^{1}H NMR.

Polymer samples were placed in a sample cell (Figure 1) which was heated by flowing hot nitrogen gas. The sample cell allows for simultaneous application of an electric field and birefringence measurement. Alignment experiments were performed well above the upper glass transition (~ 125 °C) and below the order–disorder transition (ODT) at 182 and 251 °C for SM-31 and SM-37, respectively. A vertical electric field (10–18 kV/cm) was imposed on the sample by applying a voltage to the upper electrode and grounding the lower electrode. Alignment of microstructure was monitored by birefringence measurements using a laser beam passing horizontally. The optical apparatus was described in ref 15.

III. Observations

A. Temperature and Field Dependence of Alignment Kinetics. The temperature and field dependence of the alignment rate was determined in a set of experiments. Since thermal history affects the rate of alignment (see section III.B), the thermal history was made uniform in this set of experiments; only the alignment temperature and field strength were varied. Prior to alignment, a SM-31 sample was heated well above the ODT (to erase thermal history) and then cooled at –0.5 °C/min to 175 °C. The sample was either held at that temperature or quickly cooled to 155 or 165 °C. Once the temperature was stable, a 15 kV/cm electric field was applied and the alignment tracked by monitoring the sample birefringence. The orientational order parameter, S, was calculated from eq 1.16. ($\langle \bar{\psi}^2 \rangle$ was calculated as a function of temperature from the theory of Fredrickson and Helfand.[23,24]) Figure 2a shows the evolution of S at the three temperatures. The time axis for the data at 175 °C was shifted to correct for a lag in the alignment process, presumably due to slow ordering kinetics at that temperature. (The shift was chosen so that the short-time data extrapolated to zero alignment at zero time.)

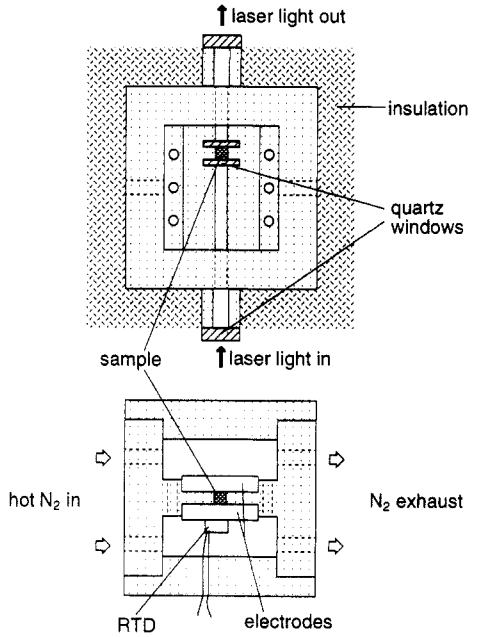

Figure 1. Top and side cross-sectional views of the sample cell. The upper electrode is not shown in the top view for clarity. The upper electrode is attached to a high-voltage source and the lower electrode is grounded. Temperature is monitored by a resistance temperature detector (RTD) attached to the lower electrode.

Alignment is slower at lower temperatures. Significantly below 155 °C no alignment could be observed on experimental time scales, presumably because of slowing down as the glass transition is approached (see below). Figure 2b shows the alignment kinetic data where the time axis has been shifted by the rheological temperature shift factor, a_T, given in the form of a WLF equation[25]

$$\log a_T = \frac{-C_1(T - T_0)}{C_2 + (T - T_0)} \tag{3.1}$$

where $C_1 = 8.03$, $C_2 = 167.89$, and the reference temperature, T_0, is 170 °C. This shift factor was determined from time–temperature superposition of high-frequency rheological measurements of the block copolymer material.[26] It compensates for the temperature dependence of molecular dynamics associated with single-chain motion. Reasonable overlap of the data is achieved, especially at short times; at later times the data often exhibit irregular jumps and are not strictly reproducible. The last datum for 155 °C also suggests that the ultimate degree of alignment may be less at that temperature. From eq 3.1 one predicts that the alignment rate at 145 °C would be

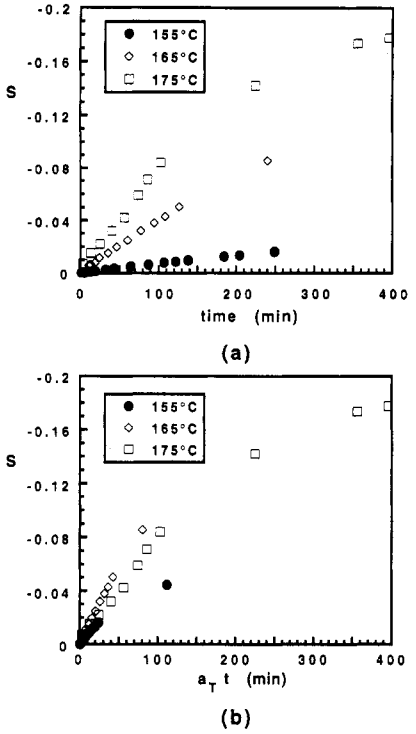

Figure 2. (a) Evolution of the orientational order parameter, S, of the lamellar microstructure in a SM-31 sample in a 15 kV/cm electric field and at three temperatures. In (b) the time axis is multiplied by the rheological temperature shift factor, a_T.

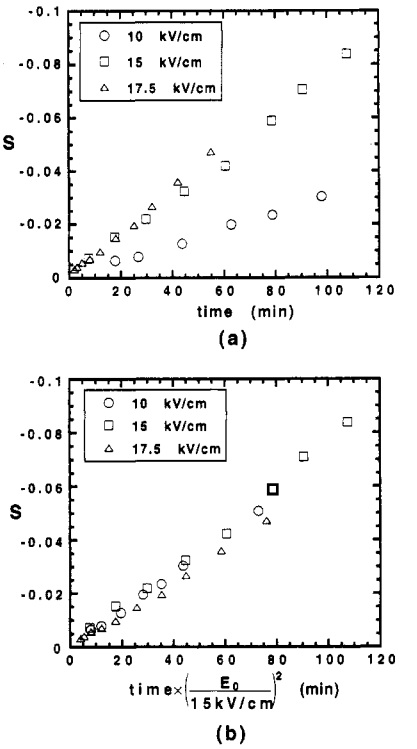

Figure 3. (a) Evolution of the orientational order parameter, S, of lamellae in a SM-31 sample at 175 °C in three electric field strengths. In (b) the time axis is reduced by the inverse square of the electric field strength.

over 4 times slower than at 155 °C and 40 times slower than at 175 °C. This explains why alignment was not observed well below 155 °C.

In a similar set of experiments, alignment of the SM-31 copolymer microstructure was performed at 175 °C but at various field strengths; the data are shown in Figure 3a. By scaling the time axis by the square of the field strength, the data are once again superimposed, as shown in Figure 3b.

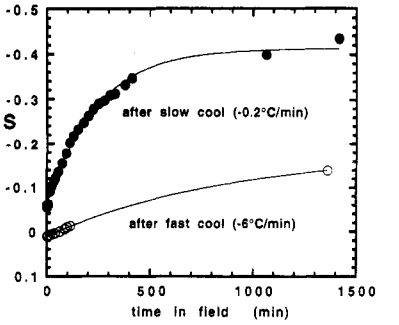

Figure 4. Evolution of the orientational order parameter, S, of lamellae in a SM-37 sample at 200 °C in a 10 kV/cm electric field. In one case, the sample was cooled slowly (–0.2 °C/min) from the disordered state just prior to alignment. In the other case the sample was cooled more rapidly (–6 °C/min). The smooth curves are best fits of the data based upon exponential relaxation.

From the optical measurements, one determines the projection of the orientation distribution onto the plane perpendicular to the optical trajectory (actually, the projection of $\langle \hat{\mathbf{e}}_q \hat{\mathbf{e}}_q \rangle$ onto that plane). A priori, one expects from field alignment a uniaxial orientation distribution about the field direction. In that case, the birefringence strength relates directly to the order parameter, S, of the orientation distribution according to eq 1.16, and the slow optical axis is in the field direction. In actual alignment experiments, the slow optical axis often slowly wandered during alignment and typically deviated about 2–10° from the field direction. SAXS patterns also verified this misalignment. The slow axis deviated much more severely at lower temperatures and for weaker field strengths. For example, for the alignment of the lamellae of SM-31 in a 15 kV/cm field, the slow axis deviated ~12° from the vertical when it was aligned at 175 °C, ~17° when aligned at 165 °C, and ~40° when aligned at 155 °C.

To rationalize the misalignments, it is important to realize that even in the absence of an applied field some macroscopic birefringence will develop. This is not unexpected; as the microstructural pattern coarsens due to the annihilation of defects, the lamellae will eventually "choose" a direction of alignment. The "choice" could be based upon symmetry-breaking agents such as aligning forces at surfaces or impurities. In fact, even though the slow optical axis that evolved during annealing in the absence of an electric field varied from sample to sample, it had a clear tendency toward horizontal alignment (i.e., horizontal lamellae). The reason for this is uncertain, but it is possibly due to surface alignment at the electrodes. This tendency is opposed by field alignment. Perhaps the ultimate directions of the optical axes represent a competition of the electric field-induced force and the tendency for horizontal alignment. This could explain why misalignment with the field is worse when the aligning field strength is smaller. Why this is also the case at low temperatures is not clear.

B. Thermal History Dependence of Alignment Kinetics. One goal of these studies was to ascertain the role of defect density on alignment kinetics. For this aspect of the study, the SM-37 material was chosen. This material has a relatively high ODT (~251 °C), and so it can be annealed at a high temperature and then supercooled to slow down the annealing process during field alignment. (For the SM-31 block copolymer, on the other hand, the accessible degree of supercooling is rather limited because of the glass transition.) Data from two alignment experiments on SM-37 at 200 °C and a 10 kV/cm field strength are shown in Figure 4. In one case, the sample was cooled at –0.2 °C/min from the disordered state to 200 °C prior to alignment, and in the other case the cooling rate was

−6 °C/min. The rate of alignment is over 10 times faster for the slowly cooled sample than the rapidly cooled sample. The data also suggest a greater ultimate alignment for the slowly cooled sample, although there are insufficient data to establish a final orientational order parameter.

The effect of annealing during the slow cool on the defect density was apparent from an optical measurement. A "minimized light intensity" measurement (described in ref 15) increases with increasing microstructural coherence length. For large coherence length, the minimum intensity scales as the square root of the coherence length.[27] For small coherence length, the scaling is more complicated. The ratio of the minimized light intensity for the slowly cooled sample to that for the rapidly cooled sample just prior to alignment at 200 °C was 5.5, indicating the coherence length was 2–3 times greater for the slowly cooled sample than for the rapidly cooled sample. An attempt was made to verify this by electron microscopy. Although micrographs were in qualitative agreement with the conclusion from the optical measurement, the variation of defect density among micrographs was too large to permit a quantitative deduction.

IV. Discussion

A. Time–Temperature–Field Superposition. The superposition of the alignment kinetic data for SM-31 by use of the rheological temperature shift factor suggests that the rate of alignment scales with single-chain dynamics. (As the glass transition is approached, the temperature shift factor, a_T, is strongly temperature dependent, and so the temperature dependence of single-chain dynamics dominates the temperature dependence of the alignment rate.) This is consistent with the conclusion in a companion paper[10] that the fundamental process involved in alignment of microstructure is movement of edge dislocations. Movement of an edge dislocation ultimately involves reorientation of single block copolymer chains.[10]

The fact that the rate of alignment scales with the square of the field strength is not surprising, since the thermodynamic driving force for alignment is proportional to the square of the field strength (see eq 1.4). On the other hand, if the rate of alignment had an even stronger field strength dependence, it could be indicative of an activated process for alignment, such as nucleation of new defect structures. The data do not point to such a process. However, they do not rule it out either, since only a small range of field strengths was explored.

It should also be noted that although alignment was quite slow for the experiments represented in Figures 2–4, the rate of alignment was much faster for the SM-37 copolymer at higher temperatures. For example, nearly complete alignment was achieved within minutes in an 18 kV/cm field at 247 °C. This relatively fast alignment is attributed to the fast chain dynamics at elevated temperatures (see eq 3.1).

An unexpected finding was the misalignment of the principal optical axes of samples which were field-aligned. The general trend was that the misalignment was lowest (~2–10°) at high temperatures and high field strengths and more severe at lower temperatures and low field strengths. It is perhaps inherent in the nature of alignment through movement of defects to result in some misalignment. For instance, the thermodynamic incentive to align lamellae that are misaligned from preferred orientations by 10° is only 3% as strong as the thermodynamic driving force for alignment of lamellae which are orthogonal to the preferred orientations. It is conceivable that the stochastic processes of biased coarsening in a field result in large domains where the microstructure is only slightly misaligned from preferred orientations. Because of the very small driving force, it would be difficult to alter their alignment. Large, "slightly misaligned" domains may have very long lifetimes.

In the absence of an applied field, coarsening of the microstructural pattern would result in some birefringence as well. This is not unexpected; as the microstructural pattern coarsens during annealing, small imbalances in the orientational distribution will be amplified. Even a globally-isotropic sample will have to choose a direction once the coherence length of the microstructure reaches the sample size. In our apparatus, samples annealed in the absence of an electric field would develop birefringence in various directions, but with a pronounced tendency for the lamellar normal to be vertical (alignment contrary to electric field alignment). It is well known that a surface induces strong local alignment.[28,29] We can only presume that the observed bias is due to surface forces. The field alignment experiments which resulted in strong misalignment of the microstructure presumably indicate conditions where the surface forces and the electric field aligning forces are comparable. We expect that these conditions are a strong function of the sample geometry and materials of construction, and so our observations are not universally applicable. Nonetheless, the observations do point to the fact that, because of competition with other forces, a minimum field strength is necessary to achieve the desired alignment.

B. Thermal History Dependence of Alignment Rate. The strong thermal history dependence of the rate of alignment for the SM-37 copolymer microstructure (see Figure 4) is quite interesting and likely reflects interactions between defects. Recall that the coherence length of the microstructure was 2–3 times higher in the slowly cooled sample, so that the number density of defects is on the order of 15–20 times greater for the rapidly cooled sample. (Here we made the approximation that the coherence length scales as the inverse cube root of the density of defects.) The extent to which the electric field induces movement of defects depends upon the mobility of these defects. It is likely that the mobility of wall defects is significantly reduced by the presence of other defects. In general, there are forces between defect structures. Consider, for instance, disclination lines. Such lines must either form complete loops or end at the edge of the sample or, more frequently, on defect walls. For example, if a disclination line ends on a defect wall, movement of the wall results in a change in the length of the disclination lines, resulting in a change in the energy associated with these lines. Also, it is often found that wall defects are perpendicular bisectors of the planes making up the lamellar patterns on each side of the wall. This is a condition of low energy for a wall defect because continuity of the lamellar periodicity in the plane of the wall can be maintained. If such a wall defect migrates to a region where the lamellar pattern is distorted, such as near a defect, this registry cannot be maintained and the energy of the wall defect will increase. Mechanisms such as these, by which the energy of a wall defect is not translation-invariant, could pin or reduce the mobility of defect walls. These issues are discussed in more detail in the companion paper.[10]

Let us consider the usefulness of electric field alignment of lamellar microstructure in an industrial process or in experimental science. There are two relevant issues, one based upon thermodynamics, the other kinetic. Thermodynamics states that an electric field does not drive the lamellar morphology to a "single-crystal-like" config-

uration. Instead the lowest energy configurations include all orientations along a ring such that the lamellar normals are perpendicular to the field direction (see eq 1.8). It is worth noting at this point that by use of a rotating electric field, or other schemes where the field changes direction, one could create a condition where there is a singular lowest energy orientation. When the time dependence of the electric field is faster than microstructural rearrangement, the microstructure will respond to the mean square field strength in three orthogonal directions. For example, by rotating a sample about an axis orthogonal to the electric field, a lamellar microstructure will be driven toward the unique orientation where the lamellar normal vector is along the rotation axis.

The data presented in this paper show that the rate of alignment is quite slow, at least in comparison to typical flow alignment processes. The most rapid alignment has been achieved at higher temperatures (alignment in less than ~10 min for SM-37 at 247 °C in an 18 kV/cm field). However, at lower temperatures and at lower field strengths, alignment requires hundreds of minutes. The slow alignment is a reflection of the small electric field-induced driving force, which is proportional to

$$\frac{\beta^2}{\epsilon_D}|\mathbf{E}_0|^2\langle\bar{\psi}^2\rangle \tag{3.2}$$

For many common block copolymers, this quantity is smaller (at the same field strength) than for the PS–PMMA copolymer studied in this report. Thus, the kinetic limitations for field alignment would be more severe for these copolymers.

In many experiments, the orientational order parameter, S, appeared to plateau well before ultimate alignment at S equal to $-1/2$, especially at lower temperatures and in unannealed samples where the defect density is high (cf. Figure 4). We speculate that this is due to trapped misaligned states. Such states would persist when energetic barriers to alignment due to defect–defect interactions are too great to be surmounted by the alignment force. The data suggest that this is more prevalent in samples that have not been annealed (i.e., where the density of defects is greater), as reflected in Figure 4, and at lower temperatures. This will impose limitations on the ultimate alignment.

It seems unlikely that alignment by an electric field can compete with well-known flow alignment methods for achieving strong alignment of lamellar microstructure. Not only is alignment in a field slow, but complete alignment is relatively difficult to achieve. However, field alignment offers means of orienting block copolymer microstructure in ways not possible by flow methods and may be desirable in molding operations for example. For instance, consider a mold with a narrow slot. The flow involved in filling the slot with a block copolymer with a lamellar morphology induces alignment of the lamellae parallel to the surfaces. If the mold is of electrically insulating construction, and a pair of opposing electrodes are embedded in the mold across the slot, an electric field can be imposed across the slot over the area of extent of the electrodes. By applying a voltage difference across the electrodes, one can induce alignment of the block copolymer microstructure in the directions orthogonal to the flow- and surface-induced alignment directions. By choosing the placement and size of electrodes, one can choose to apply the electric field-induced alignment only in desired regions of the sample.

Finally, the physics of field alignment is simpler than flow-induced alignment. (In an electric field, there is a simple body torque on the lamellar pattern as given by eq 1.8.) Because of this, field alignment may offer a convenient way to study material properties such as defect mobility and interactions between defects.

References and Notes

(1) Keller, A.; Pedemonte, E.; Willmouth, F. M. *Kolloid Z. Z. Polym.* **1970**, *238*, 385.
(2) Folkes, M. J.; Keller, A. *Polymer* **1971**, *12*, 222.
(3) Hadziioannou, G.; Mathis, A.; Skoulios, A. *Colloid Polym. Sci.* **1979**, *257*, 136.
(4) Keller, A.; Odell, J. A. In *Processing Structure and Properties of Block Copolymers*; Folkes, M. J., Ed.; Applied Science: London, 1985; p 29.
(5) Morrison, F.; Bourvellec, G. L.; Winter, H. H. *J. Appl. Polym. Sci.* **1987**, *33*, 1585.
(6) Morrison, F. A.; Winter, H. H. *Macromolecules* **1989**, *22*, 3533.
(7) Winey, K. I.; Patel, S. S.; Larson, R. G.; Watanabe, H., submitted for publication in *Macromolecules*.
(8) Koppi, K. A.; Tirrell, M.; Bates, F. S.; Almdal, K.; Colby, R. H., submitted for publication in *J. Phys. (Paris)*.
(9) Amundson, K.; Helfand, E.; Davis, D. D.; Quan, X.; Patel, S. S.; Smith, S. D. *Macromolecules* **1991**, *24*, 6546.
(10) Amundson, K.; Helfand, E.; Quan, X.; Hudson, S. D.; Smith, S. D. *Macromolecules*, in preparation.
(11) For a discussion of electrostatics and thermodynamics, see: Landau, L. D.; Lifshitz, E. M.; Pitaevskii, L. P. *Electrodynamics of Continuous Media*, 2nd ed.; Pergamon Press: New York, 1984; Vol. 8, pp 44–51. Jackson, J. D. *Classical Electrodynamics*, 2nd ed.; John Wiley & Sons: New York, 1975; pp 158–162.
(12) The effect of dynamic fluctuations is separated from the effect of the composition pattern, $\bar{\psi}$, associated with the ordered phase. Since the dynamic fluctuations have short correlation lengths for the copolymers in this study, they will not significantly couple to an electric field. The stationary composition pattern can have a much larger correlation length and can couple strongly to an electric field.
(13) The meanings of the overhead bar and angular brackets are the same as in ref 10. Unfortunately, we reversed their usage in ref 15.
(14) Lodge, T. P.; Fredrickson, G. H., submitted for publication in *Macromolecules*.
(15) Amundson, K.; Helfand, E.; Quan, X.; Patel, S. S.; Smith, S. D. *Macromolecules* **1992**, *25*, 1935.
(16) Born, M.; Wolf, E. *Principles of Optics*; Pergamon Press: New York, 1959.
(17) Landau, L. D.; Lifshitz, E. M.; Pitaevskii, L. P. *Electrodynamics of Continuous Media*, 2nd ed.; Pergamon Press: New York, 1984; Vol. 8, p 460.
(18) Balsara, N. P.; Perahia, D.; Safinya, C. R.; Tirrell, M.; Lodge, T. P. *Macromolecules* **1992**, *25*, 3896.
(19) Balsara, N. P.; Garetz, B. A.; Dai, H. J. *Macromolecules* **1992**, *25*, 6072.
(20) Milner, S. T., submitted for publication.
(21) The "region of coherence" is a concept we have adopted for convenience. Within a "region of coherence", the microstructure is considered uniform and uncorrelated with the surrounding microstructure. In the paradigm of a polycrystalline texture, a region of coherence would be a single grain. In reality, microstructure orientation exhibits slow, continuous changes as well as sharp changes at defects.
(22) Michel, P.; Dugas, J.; Cariou, J. M.; Martin, L. *J. Macromol. Sci., Phys.* **1986**, *B25*, 379. Data for 578-nm light are given. We make no correction for differences in refractive index between 578-nm and 632.8-nm light.
(23) Fredrickson, G. H.; Helfand, E. *J. Chem. Phys.* **1987**, *87*, 697.
(24) Fredrickson, G. H.; Binder, K. *J. Chem. Phys.* **1989**, *91*, 7265.
(25) Ferry, J. D. *Viscoelastic Properties of Polymers*, 3rd ed.; Wiley: New York, 1980.
(26) Patel, S. S.; Helfand, E.; Quan, X.; Amundson, K. R.; Smith, S. D. *Macromolecules*, in preparation.
(27) When the coherence length is sufficiently large, the minimized light intensity scales as the square root of the coherence length (see reference note 32 of ref 15). The square-root relation between the coherence length and the minimized light intensity is at best semiquantitative and is used here as an approximation.
(28) Russell, T. P.; Coulon, G.; Deline, V. R.; Miller, D. C. *Macromolecules* **1989**, *22*, 4600 and references therein.
(29) Coulon, G.; Ausserre, D.; Russell, T. P. *J. Phys. (Paris)* **1990**, *51*, 777 and references therein.